Supporting Information for

Strong Dipolar Effects on an Octupolar Luminiscent Chromophore: Implications on their Linear and Nonlinear Optical Properties

Arturo Jiménez-Sánchez,†,* Itzel Isunza Manrique,§ Gabriel Ramos-Ortiz,§ Jesús Rodríguez-Romero,† Norberto Farfán† and Rosa Santillan‡

† Facultad de Química, Universidad Nacional Autónoma de México, México D.F. No. 04510, México.

§ Centro de Investigaciones en Óptica, CIO, Apdo., Postal 1-948, 37000 León Gto, México.

‡ Departamento de Química, Centro de Investigación y de Estudios Avanzados del IPN, Apdo. Postal 14740, México, D. F. 07000, México.

*To whom correspondence should be addressed: arturo@cinvestav.mx

Chemical Characterization

2-bromo-9,9-dioctylfluorene (**1**). A solution of 1-bromooctane (8.66 g, 44.9 mmol) in 5 ml of DMSO was added to a mixture of 2-bromofluorene (5.00 g, 20.40 mmol) and KOH (8.16 g, 204 mmol) in 35 ml of DMSO. The reaction was stirred for 15 hours at 60ºC.[1] The completion of the reaction was verified by TLC. The organic phase was extracted with 20 ml of ethyl acetate and was washed with water (3 x 20 ml). The resulting organic solution was then dried over anhydrous Na_2SO_4 and the solvent was eliminated in vacuo. The residue was redissolved with hexane and subjected to column chromatography on silica using hexane as eluent to afford a yellow oil (**1**) in 83% yield (2.6 g). ^{1}H NMR (500 MHz, $CDCl_3$): δ 7.69-7.67 (m, 1H), 7.56 (d, ^3J = 8 Hz, 1H), 7.49 (d, ^4J = 1.8 Hz, 1H), 7.46 (dd, ^3J = 8 Hz, ^4J = 1.8 Hz, 1H), 7.35-7.32 (m, 3H), 1.99-1.94 (m, 4H), 1.26-1.06 (m, 20H), 0.85 (t, J=10 Hz, 6H), 0.67-0.6 (m, 4H). ^{13}C NMR (125 MHz, $CDCl_3$): δ 153.1, 150.4, 140.2, 140.1, 130.0, 127.5, 127.0, 126.2, 122.9, 121.13, 121.11, 119.8, 55.4, 40.4, 31.9, 30.1, 29.34, 29.32, 23.8, 22.7, 14.2. IR (ν_{max}/cm^{-1}) 2923-2852 (C-H_{alkyl}), 1465 (C-H deformations), 736 (C-Br). ESI-MS calculated for $C_{29}H_{42}Br$ $[M+H]^+$ 469.2464, found 469.2466 $[M+H]^+$ (ppm error of 0.3426).

2-trimethylsilylethynyl-9,9-dioctylfluorene (**2**). Compound **1** (3.02 g, 6.43 mmol) was dissolved in DIPA freshly destilled under N_2. After, $Pd(O_2CCH_3)_2$ (86 mg, 0.38 mmol), CuI (86 mg, 0.45 mmol) and PPh_3 (0.17 g, 0.64 mmol) were added to the solution. The reaction was cooled to 0°C and then ethynyltrimethylsilane (4.58 g, 46.63 mmol) was added. The reaction was stirred for 2 h. The resulting mixture was then heated at 85°C overnight. The reaction progress was monitored by TLC, the DIPA was evaporated under vacuum. The residue was extracted with 10 ml of diethyl ether and (3 x 10 mL) of water. The solvent

was eliminated under vacuum, the residue was redissolved with ethyl acetate and subjected to column chromatography on silica using hexane as eluent to afford a yellow oil of **2** in 83% yield (2.6 g). ^{1}H NMR (500 MHz, $CDCl_3$): δ 7.68-7.66(m, 1H), 7.61(d, ^{3}J=7.9 Hz, 1H), 7.45(dd, ^{3}J=7.9 Hz ^{4}J=1.3 Hz, 1H), 7.43(s, 1H), 7.33-7.31(m, 3H), 1.94(t, *J*=8.6, 4H), 1.23-1.02(m, 20H), 0.82(t, J=10, 6H), 0.62-0.51(m, 4H), 0.29(s, 9H). ^{13}C NMR (125 MHz, $CDCl_3$): δ 151.1, 150.6, 141.7, 140.4, 131.2, 127.6, 126.9, 126.3, 122.9, 121.2, 120.1, 119.5, 106.3, 93.8, 55.2, 40.5, 31.8, 30.1, 29.3, 23.7, 22.6, 14.1, 0.3.

2-ethynyl-9,9-dioctylfluorene (**3**). Compound **3** was prepared following the metodology reported in the literature. ^{1}H NMR (500 MHz, $CDCl_3$): δ = 7.69-7.67(m, 1H), 7.64(d, *J*=10 Hz, 1H), 7.48-7.46(m, 2H), 7.35-7.3(m, 3H), 3.13(s, 1H), 1.94(t, *J*=10 Hz, 4H), 1.25-1.02(m, 20H), 0.82(t, *J*=10 Hz, 6H), 0.63-0.52(m, 4H). ^{13}C NMR (125 MHz, $CDCl_3$): δ 151.1, 150.7, 142, 140.3, 131.1, 127.7, 126.9, 126.6, 122.9, 120.19, 120.15, 119.6, 84.8, 76.9, 55.2, 40.3, 31.8, 30, 29.3, 23.7, 22.6, 14.1. IR (ν_{max}/cm^{-1}) 3309 (alkyne C-H stretching), 2924 (C-H stretching), 2360 (C-C triple bond), 2105 (C-C triple bond stretching), 1450 (C-H deformations). ESI-MS calculated for $C_{31}H_{43}$ $[M+H]^+$ 415.3359, found 415.3359 $[M+H]^+$ (ppm error of -0.0677).

2-(4-ethynylbenzonitrile)-9,9-dioctylfluorene (**DS**). Compound **3** (1.00 g, 2.41 mmol), 4-bromobenzonitrile (0.44 g, 2.41 mmol), CuI (0.0184 g, 0.097 mmol) and $Pd(Cl)_2(PPh_3)_2$ (0.0676g, 0.097 mmol) were mixed, then TEA (30 mL) freshly destilled were added under N_2. The resulting mixture was then heated at 85°C overnight. The reaction progress was monitored by TLC, the TEA was evaporated under vacuum. The residue was extracted with 10 ml of ethyl acetate and (3 x 10 mL) of water. The solvent was eliminated under vacuum, the residue was redissolved with ethyl acetate and loaded to a silica column

chromatography using hexane as eluent to afford a crystalline solid of **DS** in 81% yield (1.01 g). ^{1}H NMR (500 MHz, C_6D_6): δ = 7.68 (1H, d, J = 0.85 Hz, H1), 7.50-7.49 (1H, m, H5), 7.48-7.47 (1H, m, H3), 7.38 (1H, d, J = 7.7 Hz, H4), 7.16-7.13 (3H, m, H6, H7, H8), 7.02 (2H, d, H17), 6.75 (2H, d, H18), 1.92 (4H, q, J = 7.0, 2.6 Hz, H21), 1.21-0.95 (20H, m), 0.76 (Me, t, J = 7.15 Hz, 6H), 0.73-0.66 (m, 4H). ^{13}C NMR (125 MHz, C_6D_6): δ 151.1 (C10), 142.5 (C11), 140.4 (C13), 131.8 (C18), 131.6 (C17), 131.0 (C3), 128.0 (C8), 127.2 (C7), 126.1 (C1), 122.9 (C6), 120.9 (CN), 120.4 (C5), 120.1 (C4), 118.1 (C19), 111.7 (C16), 94.8 (C14), 88.4 (C15), 55.3 (C9), 40.5 (C21), 31.9, 30.1, 29.3, 23.9, 22.8, 14.1 (Me). m.p.: 94–96ºC; IR (ν_{max}/cm^{-1}) 2951, 2923, 2850 (aromatic C-H stretching), 2850 (aliphatic C-H stretching), 2226 (CN stretching), 2205, (C-C triple bond stretching), 1601, 835. ESI-MS calculated for $C_{38}H_{46}N_1$ $[M+H]^+$, 516.3624 found 516.3625 $[M+H]^+$ (ppm error of 0.0440).

2,4,6-tris-[2-(4-ethynylbenzonitrile)-9,9-dioctylfluorene]-1,3,5-triazine (**OS**). This compound was prepared by two methodologies. Methodology A: Compound **3** (0.100 g, 0.25 mmol), 2,4,6-*tris*-(4-iodophenyl)-1,3,5-trizine (0.055 g, 0.08 mmol), CuI (0.040 g, 0.097 mmol) and $Pd(Cl)_2(PPh_3)_2$ (0.169g, 0.097 mmol) were mixed in toluene, then TEA (30 mL) freshly destilled were added under N_2. The resulting mixture was then heated at 85°C overnight. The reaction progress was monitored by TLC, the TEA was evaporated under vacuum. The residue was extracted with 10 ml of ethyl acetate and (3 x 10 mL) of water. The solvent was eliminated under vacuum, the residue was redissolved with ethyl acetate and loaded to a silica column chromatography using hexane as eluent to afford a dark yellow solid of **OS** in 64% yield (0.24 g). Methodology B: A solid-state nitrile cyclotrimerization reaction of compound **DS** was catalized by $ZnCl_2$ lewis acid at 300°C

for 48 hours. Compound **DS** and $ZnCl_2$ in a 3 : 1 molar ratio were filled into an ampoule under nitrogen and sealed under vacuum at this conditions, compound **OS** was obtained in poor 22% yield (0.08 g). However, the compound was easier to purify by simple extraction with 10 ml of methylene chloride (3 x 10 mL) in water. ^{1}H NMR (500 MHz, C_6D_6): δ 8.81 (d), 7.80 (d,) 7.74-7.70 (m,) 7.62-7.60 (m,) 7.39-7.34 (m,) 2.03 (t,) 1.28-1.09 (m,) 0.85 (t,) 0.74-0.59 (m). RMN de 13C (125 MHz; C6D6): δ 171.2, 151.2, 151.0, 142.0, 140.5, 135.6, 131.9, 131.0, 129.1, 128.0, 127.0, 126.2, 123.0, 121.1, 120.2, 119.9, 93.8, 89.4, 55.3, 40.5, 31.9, 30.2, 29.4, 23.9, 22.7, 14.2. m.p.: 357–359ºC; IR (ν_{max}/cm^{-1}) 2954, 2925, 2853 (aromatic C-H stretching), 2163 (C≡C triple bond stretching). FAB-MS calculated $C_{114}H_{135}N_3$ 1546.06 [M], found 1546.1. Anal. Calc. for $C_{114}H_{135}N_3$: C, 88.49; H, 8.79; N, 2.72. Found: C, 88.60; H, 8.65; N, 2.94.

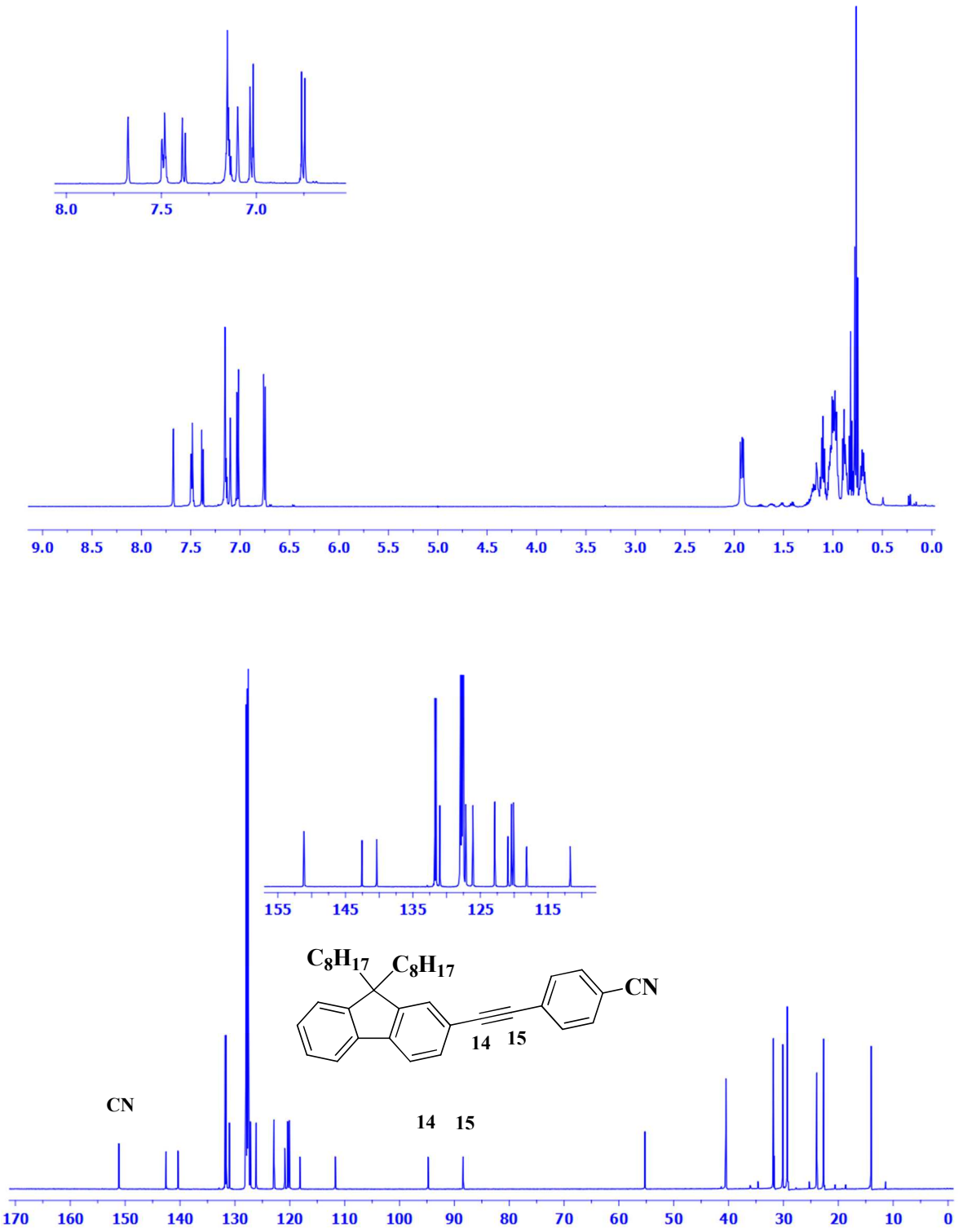

Figure S8A. ^{1}H and ^{13}C NMR spectra of compound **DS** in $CDCl_3$.

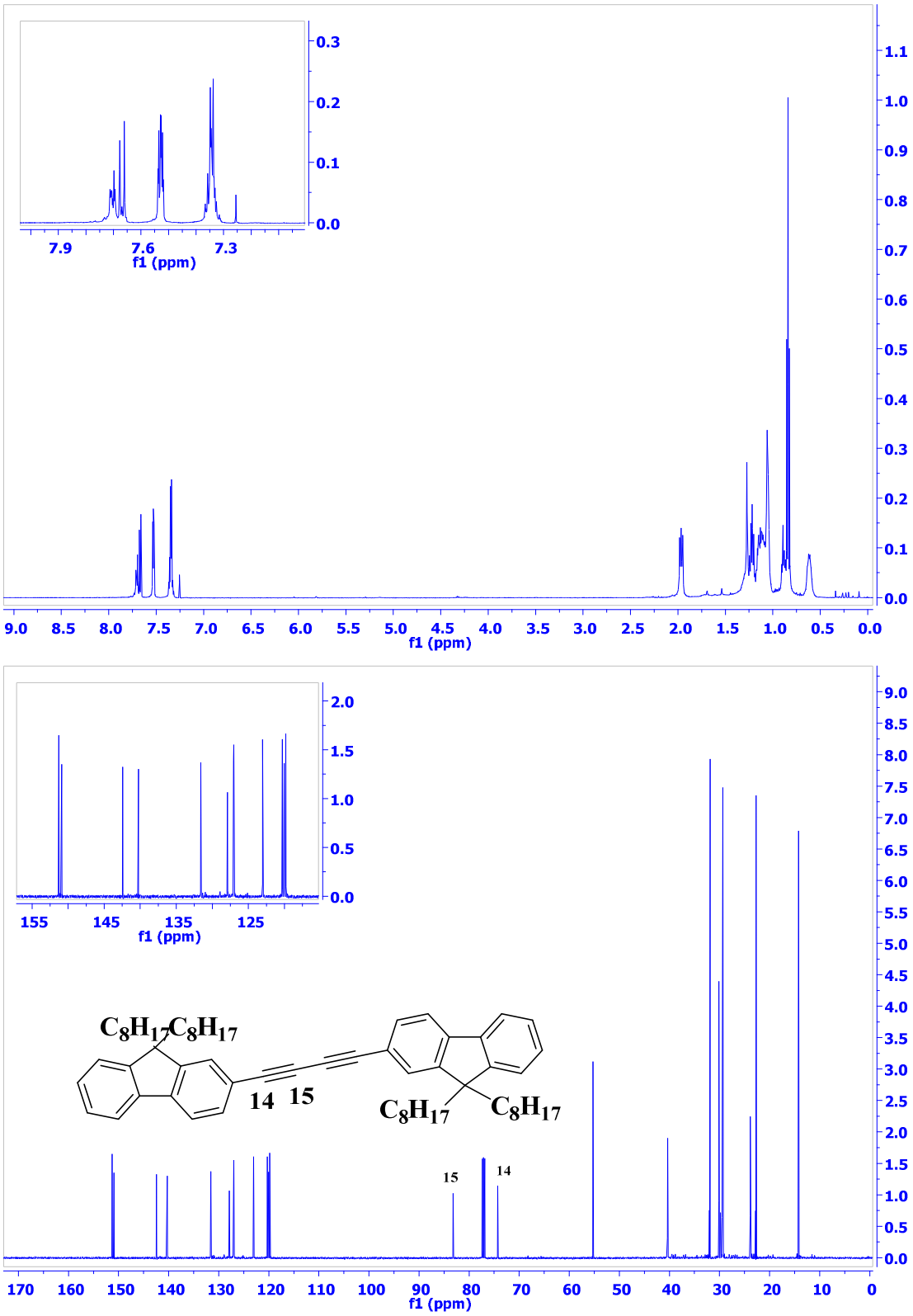

Figure S8B. ^{1}H and ^{13}C NMR spectra of compound **2DS** in $CDCl_3$.

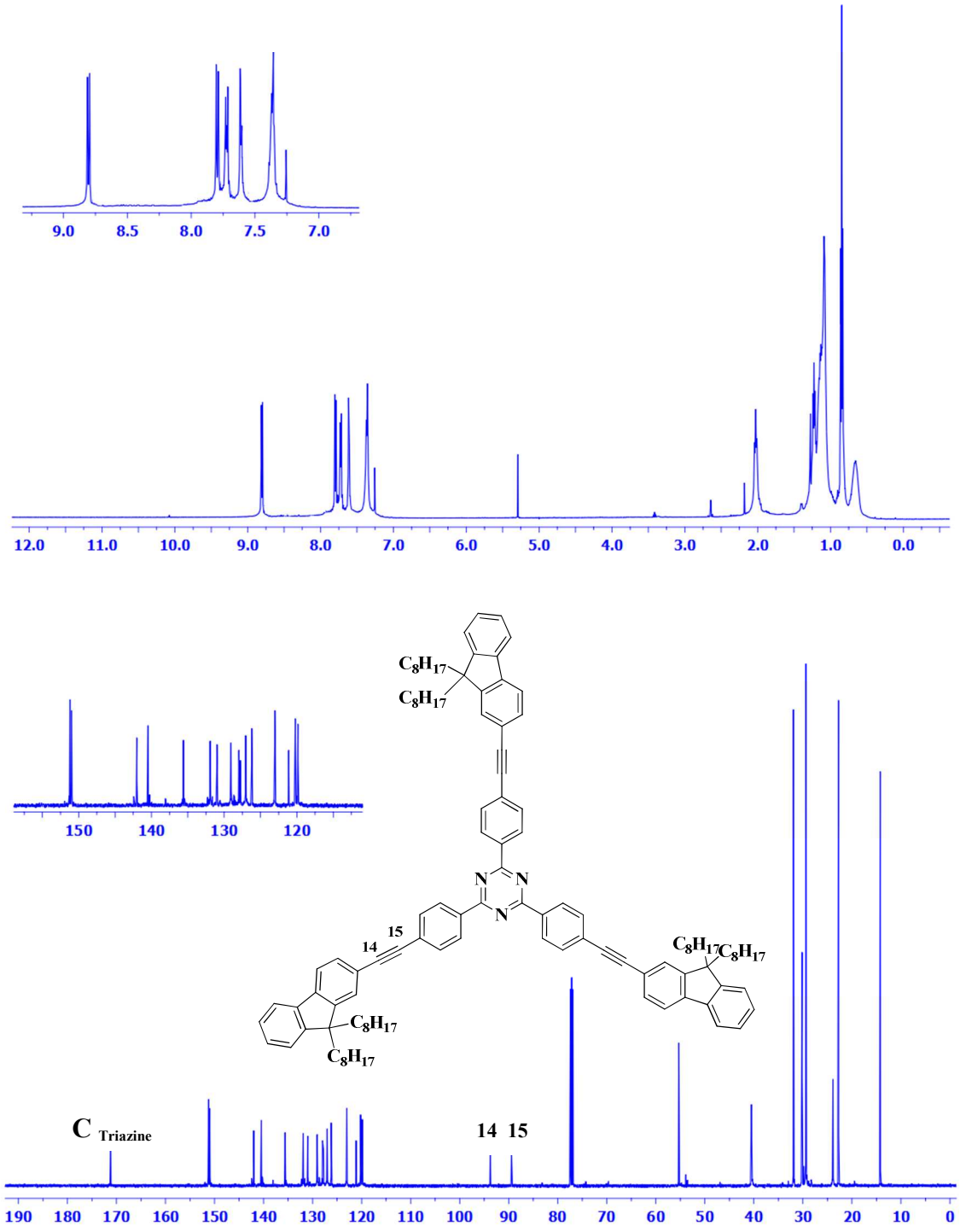

Figure S8C. ^{1}H and ^{13}C NMR spectra of compound **OS** in $CDCl_3$.

X-ray diffraction analysis and data collection. Single crystals of compound **DS** suitable for X-ray diffraction were obtained by slow evaporation from a saturated chloroform solution at room temperature. The crystal data were recorded on an Enraf Nonius Kappa-CCD (λ MoKα= 0.71073 Å, graphite monochromator, T=298K). Each crystal was mounted on conventional MicroLoops™. All reflection data set were corrected for Lorentz and polarization effects. Structure solution and refinement were carried out with the SHELXS-2014 and SHELXL-2014 packages [Sheldrick, G. M. Program for Crystal Structure Solution. University of Göttingen: Göttingen, Germany, 1997. *Acta Cryst., Sect. A: Found. Crystallogr.*, **2008**, *64*, 112–122.]; WinGX v2014.1 software was used to prepare material for publication [Farrugia, L. J. *Appl. Cryst.*, **1999**, *32*, 837–838.]. Full-matrix least-squares refinement was carried out by minimising $(Fo^2 - Fc^2)^2$. All non-hydrogen atoms were refined anisotropically. H atoms attached to C atoms were placed in geometrically idealized positions and refined as riding on their parent atoms, with C–H = 0.93–0.97 Å and with U_{iso}(H) = 1.2U_{eq}(C) for aromatic and methylene groups, and U_{iso}(H) = 1.5U_{eq}(C) for methyl groups. C63 C64 C65 C66 C67 C68 and C63a C64a C65a C66a C67a C68a are disordered over two sites with occupancies 0.71:0.29, while C73 C74 C75 C76 and C73a C74a C75a C76a are disordered over two sites with occupancies 0.50:0.50.

Crystal data and experimental details of the structure determination of **DS** are listed in Table S1, Supplementary Information. The crystallographic data for the structure reported in this paper has been deposited with the Cambridge Crystallographic Data Centre as supplementary publication no. CCDC 1443732. Copies of the data can be obtained free of charge on application to CCDC, 12 Union Road, Cambridge, CB2 1EZ, UK (fax: (+44) 1223-336-033, e-mail: deposit@ccdc.cam.ac.uk).

Table S1. Table S1. Crystal data and structure refinement for **DS**.

Identification code	**DS**	
Empirical formula	C38 H45 N	
Formula weight	515.75	
Temperature	298(2) K	
Wavelength	0.71073 Å	
Crystal system	Triclinic	
Space group	P -1	
Unit cell dimensions	a = 11.4197(3) Å	α= 88.9120(10)°.
	b = 14.4372(3) Å	β= 80.8000(10)°.
	c = 21.8529(5) Å	γ = 67.9940(10)°.
Volume	3294.10(14) $Å^3$	
Z	4	
Density (calculated)	1.040 Mg/m^3	
Absorption coefficient	0.059 mm^{-1}	
F(000)	1120	
Crystal size	0.350 x 0.300 x 0.125 mm^3	
Theta range for data collection	3.514 to 25.350°.	
Index ranges	-13<=h<=13, -17<=k<=17, -26<=l<=26	
Reflections collected	36813	
Independent reflections	11750 [R(int) = 0.0849]	
Completeness to theta = 25.242°	97.3 %	
Refinement method	Full-matrix least-squares on F^2	
Data / restraints / parameters	11750 / 21 / 681	
Goodness-of-fit on F^2	1.026	
Final R indices [I>2sigma(I)]	R1 = 0.1407, wR2 = 0.4605	
R indices (all data)	R1 = 0.2016, wR2 = 0.5626	
Extinction coefficient	n/a	
Largest diff. peak and hole	0.527 and -0.438 $e.Å^{-3}$	

Atomic coordinates (x 10^4) and equivalent isotropic displacement parameters ($Å^2$x 10^3) for **DS**. U(eq) is defined as one third of the trace of the orthogonalized U^{ij} tensor.

	x	y	z	U(eq)
C(1)	1621(6)	-3743(5)	7836(3)	116(2)
C(2)	2037(4)	-2975(3)	7583(2)	89(1)
C(3)	1344(5)	-1975(4)	7754(3)	120(2)
C(4)	1754(6)	-1250(4)	7522(3)	119(2)
C(5)	2903(5)	-1498(4)	7111(2)	97(1)
C(6)	3597(5)	-2489(3)	6972(2)	97(1)
C(7)	3163(6)	-3210(4)	7209(3)	127(2)
C(8)	3377(5)	-756(4)	6878(2)	97(1)
C(9)	3847(5)	-168(3)	6662(2)	91(1)
C(10)	4428(4)	473(3)	6381(2)	84(1)
C(11)	5262(5)	161(3)	5815(2)	91(1)
C(12)	5851(5)	747(3)	5519(2)	90(1)
C(13)	5622(4)	1686(3)	5779(2)	80(1)
C(14)	4831(4)	1998(3)	6356(2)	79(1)
C(15)	4228(4)	1415(3)	6654(2)	84(1)
C(16)	6087(4)	2460(3)	5557(2)	91(1)
C(17)	6865(5)	2509(5)	5007(3)	115(2)
C(18)	7134(7)	3337(6)	4899(4)	145(2)
C(19)	6644(8)	4146(7)	5316(5)	156(3)
C(20)	5873(7)	4118(4)	5857(3)	131(2)
C(21)	5594(5)	3263(4)	5987(3)	101(1)
C(22)	4786(5)	3037(3)	6548(2)	99(1)
C(23)	3468(6)	3811(4)	6707(3)	113(2)
C(24)	2653(5)	4005(4)	6206(3)	112(2)
C(25)	1404(6)	4928(4)	6396(3)	117(2)
C(26)	516(5)	5159(4)	5960(3)	117(2)
C(27)	-697(5)	6087(4)	6155(3)	122(2)
C(28)	-1682(5)	6260(4)	5754(3)	110(2)
C(29)	-2889(5)	7151(4)	5938(3)	111(2)
C(30)	-3845(6)	7232(5)	5536(3)	133(2)
C(31)	5613(8)	2944(7)	7089(3)	151(3)
C(32)	5055(9)	2824(7)	7694(5)	171(3)
C(33)	5914(7)	2863(6)	8187(3)	131(2)
C(34)	7135(7)	1991(5)	8169(3)	124(2)
C(35)	7831(7)	1924(6)	8703(3)	128(2)
C(36)	9090(9)	1001(6)	8635(3)	141(2)
C(37)	9810(10)	875(9)	9147(4)	168(3)
C(38)	10933(10)	-28(8)	9102(4)	162(3)
N(1)	1331(6)	-4376(4)	8031(3)	151(2)
C(39)	-2814(7)	15001(4)	7313(3)	121(2)
C(40)	-1664(5)	14343(3)	7548(3)	103(2)
C(41)	-891(6)	13454(4)	7215(3)	120(2)
C(42)	173(6)	12840(4)	7429(3)	122(2)
C(43)	517(4)	13082(3)	7969(2)	94(1)
C(44)	-272(5)	13979(4)	8280(3)	111(2)
C(45)	-1340(5)	14584(4)	8081(3)	113(2)
C(46)	1629(5)	12423(4)	8187(2)	102(2)

C(47)	2543(5)	11860(4)	8381(2)	96(1)
C(48)	3647(4)	11181(3)	8602(2)	88(1)
C(49)	4072(5)	11442(4)	9119(2)	103(2)
C(50)	5149(5)	10800(4)	9323(2)	100(1)
C(51)	5833(4)	9884(3)	9023(2)	80(1)
C(52)	5403(4)	9608(3)	8510(2)	73(1)
C(53)	4334(4)	10244(3)	8302(2)	84(1)
C(54)	6989(4)	9072(3)	9126(2)	83(1)
C(55)	7773(6)	8953(5)	9581(2)	108(2)
C(56)	8835(5)	8100(6)	9580(3)	114(2)
C(57)	9125(5)	7342(5)	9137(3)	111(2)
C(58)	8363(4)	7423(3)	8684(2)	92(1)
C(59)	7280(4)	8294(3)	8687(2)	80(1)
C(60)	6303(4)	8569(3)	8254(2)	79(1)
C(61)	5591(4)	7837(3)	8291(2)	89(1)
C(62)	4920(5)	7740(4)	8923(2)	101(1)
C(69)	6908(4)	8580(3)	7573(2)	86(1)
C(70)	7541(5)	9321(4)	7440(2)	96(1)
C(71)	8294(6)	9223(4)	6801(2)	113(2)
C(72)	8837(7)	9994(5)	6660(3)	133(2)
N(2)	-3711(6)	15516(4)	7160(3)	150(2)
C(63)	4310(20)	7020(18)	8910(8)	166(2)
C(64)	3710(17)	6688(10)	9504(7)	166(2)
C(65)	3330(13)	5798(10)	9431(5)	166(2)
C(66)	2628(12)	5546(7)	10021(5)	166(2)
C(67)	2544(13)	4519(8)	10055(5)	166(2)
C(68)	1812(12)	4400(10)	9560(5)	166(2)
C(63A)	4340(40)	6850(40)	8883(19)	166(2)
C(64A)	3500(30)	6930(20)	9530(20)	166(2)
C(65A)	2630(20)	6351(15)	9605(16)	166(2)
C(66A)	3430(20)	5240(16)	9502(16)	166(2)
C(67A)	2810(20)	4471(18)	9518(14)	166(2)
C(68A)	1650(30)	5080(20)	9984(13)	166(2)
C(73)	9740(20)	9736(14)	6042(7)	184(3)
C(74)	10533(16)	10323(10)	5816(9)	184(3)
C(75)	10091(15)	11466(10)	5823(10)	184(3)
C(76)	11281(17)	11686(15)	5551(10)	184(3)
C(73A)	9640(30)	10101(15)	6059(7)	184(3)
C(74A)	9946(18)	11037(13)	6078(8)	184(3)
C(75A)	11016(18)	10933(11)	5540(8)	184(3)
C(76A)	10560(20)	12067(11)	5570(10)	184(3)

Selected bond lengths [Å] and angles [°] for **DS**.

C(1)-N(1)	1.137(7)
C(1)-C(2)	1.432(8)
C(2)-C(7)	1.335(7)
C(2)-C(3)	1.386(7)
C(3)-C(4)	1.357(8)
C(3)-H(3)	0.9300
C(4)-C(5)	1.392(8)
C(4)-H(4)	0.9300
C(5)-C(6)	1.363(7)
C(5)-C(8)	1.423(7)
C(6)-C(7)	1.372(7)
C(6)-H(6)	0.9300
C(7)-H(7)	0.9300
C(8)-C(9)	1.216(6)
C(9)-C(10)	1.409(6)
C(10)-C(11)	1.400(6)
C(10)-C(15)	1.418(6)
C(11)-C(12)	1.361(6)
C(11)-H(11)	0.9300
C(12)-C(13)	1.395(6)
C(12)-H(12)	0.9300
C(13)-C(14)	1.401(6)
C(13)-C(16)	1.452(6)
C(14)-C(15)	1.370(6)
C(14)-C(22)	1.546(6)
C(15)-H(15)	0.9300
C(16)-C(21)	1.389(7)

C(16)-C(17)	1.393(7)	C(38)-H(38B)	0.9600
C(17)-C(18)	1.349(9)	C(38)-H(38C)	0.9600
C(17)-H(17)	0.9300	C(39)-N(2)	1.115(7)
C(18)-C(19)	1.376(11)	C(39)-C(40)	1.467(9)
C(18)-H(18)	0.9300	C(40)-C(45)	1.366(8)
C(19)-C(20)	1.368(10)	C(40)-C(41)	1.392(8)
C(19)-H(19)	0.9300	C(41)-C(42)	1.357(8)
C(20)-C(21)	1.398(7)	C(41)-H(41)	0.9300
C(20)-H(20)	0.9300	C(42)-C(43)	1.390(8)
C(21)-C(22)	1.520(8)	C(42)-H(42)	0.9300
C(22)-C(23)	1.491(7)	C(43)-C(44)	1.384(7)
C(22)-C(31)	1.601(9)	C(43)-C(46)	1.419(7)
C(23)-C(24)	1.504(8)	C(44)-C(45)	1.340(7)
C(23)-H(23A)	0.9700	C(44)-H(44)	0.9300
C(23)-H(23B)	0.9700	C(45)-H(45)	0.9300
C(24)-C(25)	1.547(7)	C(46)-C(47)	1.193(7)
C(24)-H(24A)	0.9700	C(47)-C(48)	1.426(7)
C(24)-H(24B)	0.9700	C(48)-C(53)	1.396(6)
C(25)-C(26)	1.446(8)	C(48)-C(49)	1.408(7)
C(25)-H(25A)	0.9700	C(49)-C(50)	1.370(7)
C(25)-H(25B)	0.9700	C(49)-H(49)	0.9300
C(26)-C(27)	1.529(8)	C(50)-C(51)	1.373(6)
C(26)-H(26A)	0.9700	C(50)-H(50)	0.9300
C(26)-H(26B)	0.9700	C(51)-C(52)	1.413(5)
C(27)-C(28)	1.481(8)	C(51)-C(54)	1.446(6)
C(27)-H(27A)	0.9700	C(52)-C(53)	1.364(6)
C(27)-H(27B)	0.9700	C(52)-C(60)	1.520(5)
C(28)-C(29)	1.495(7)	C(53)-H(53)	0.9300
C(28)-H(28A)	0.9700	C(54)-C(59)	1.398(6)
C(28)-H(28B)	0.9700	C(54)-C(55)	1.408(7)
C(29)-C(30)	1.478(8)	C(55)-C(56)	1.367(8)
C(29)-H(29A)	0.9700	C(55)-H(55)	0.9300
C(29)-H(29B)	0.9700	C(56)-C(57)	1.383(9)
C(30)-H(30A)	0.9600	C(56)-H(56)	0.9300
C(30)-H(30B)	0.9600	C(57)-C(58)	1.394(7)
C(30)-H(30C)	0.9600	C(57)-H(57)	0.9300
C(31)-C(32)	1.411(11)	C(58)-C(59)	1.394(6)
C(31)-H(31A)	0.9700	C(58)-H(58)	0.9300
C(31)-H(31B)	0.9700	C(59)-C(60)	1.512(6)
C(32)-C(33)	1.584(11)	C(60)-C(69)	1.539(6)
C(32)-H(32A)	0.9700	C(60)-C(61)	1.551(6)
C(32)-H(32B)	0.9700	C(61)-C(62)	1.500(7)
C(33)-C(34)	1.483(9)	C(61)-H(61A)	0.9700
C(33)-H(33A)	0.9700	C(61)-H(61B)	0.9700
C(33)-H(33B)	0.9700	C(62)-C(63)	1.45(2)
C(34)-C(35)	1.495(8)	C(62)-C(63A)	1.67(6)
C(34)-H(34A)	0.9700	C(62)-H(62A)	0.9700
C(34)-H(34B)	0.9700	C(62)-H(62B)	0.9700
C(35)-C(36)	1.539(10)	C(69)-C(70)	1.501(6)
C(35)-H(35A)	0.9700	C(69)-H(69A)	0.9700
C(35)-H(35B)	0.9700	C(69)-H(69B)	0.9700
C(36)-C(37)	1.462(10)	C(70)-C(71)	1.498(7)
C(36)-H(36A)	0.9700	C(70)-H(70A)	0.9700
C(36)-H(36B)	0.9700	C(70)-H(70B)	0.9700
C(37)-C(38)	1.437(12)	C(71)-C(72)	1.469(8)
C(37)-H(37A)	0.9700	C(71)-H(71A)	0.9700
C(37)-H(37B)	0.9700	C(71)-H(71B)	0.9700
C(38)-H(38A)	0.9600	C(72)-C(73A)	1.519(2)

Selected torsion angles [°] for **DS**.

C(7)-C(2)-C(3)-C(4)	3.8(9)
C(1)-C(2)-C(3)-C(4)	178.8(6)
C(2)-C(3)-C(4)-C(5)	-1.2(10)
C(3)-C(4)-C(5)-C(6)	-1.8(9)
C(3)-C(4)-C(5)-C(8)	-177.8(5)
C(4)-C(5)-C(6)-C(7)	2.2(8)
C(8)-C(5)-C(6)-C(7)	178.1(5)
C(3)-C(2)-C(7)-C(6)	-3.5(9)
C(1)-C(2)-C(7)-C(6)	-178.5(5)
C(5)-C(6)-C(7)-C(2)	0.5(10)
C(9)-C(10)-C(11)-C(12)	179.8(4)
C(15)-C(10)-C(11)-C(12)	-1.7(6)
C(10)-C(11)-C(12)-C(13)	-0.3(7)
C(11)-C(12)-C(13)-C(14)	2.8(6)
C(11)-C(12)-C(13)-C(16)	-178.1(4)
C(12)-C(13)-C(14)-C(15)	-3.3(6)
C(16)-C(13)-C(14)-C(15)	177.3(4)
C(12)-C(13)-C(14)-C(22)	177.6(4)
C(16)-C(13)-C(14)-C(22)	-1.8(5)
C(13)-C(14)-C(15)-C(10)	1.4(6)
C(22)-C(14)-C(15)-C(10)	-179.7(4)
C(11)-C(10)-C(15)-C(14)	1.1(6)
C(9)-C(10)-C(15)-C(14)	179.6(4)
C(12)-C(13)-C(16)-C(21)	-179.4(5)
C(14)-C(13)-C(16)-C(21)	-0.2(5)
C(12)-C(13)-C(16)-C(17)	2.6(8)
C(14)-C(13)-C(16)-C(17)	-178.2(5)
C(21)-C(16)-C(17)-C(18)	0.1(8)
C(13)-C(16)-C(17)-C(18)	178.0(5)
C(16)-C(17)-C(18)-C(19)	-0.9(11)
C(17)-C(18)-C(19)-C(20)	0.6(13)
C(18)-C(19)-C(20)-C(21)	0.5(12)
C(17)-C(16)-C(21)-C(20)	0.9(8)
C(13)-C(16)-C(21)-C(20)	-177.3(5)
C(17)-C(16)-C(21)-C(22)	-179.7(4)
C(13)-C(16)-C(21)-C(22)	2.1(5)
C(19)-C(20)-C(21)-C(16)	-1.3(9)
C(19)-C(20)-C(21)-C(22)	179.5(6)
C(16)-C(21)-C(22)-C(23)	-126.5(5)
C(20)-C(21)-C(22)-C(23)	52.8(7)
C(16)-C(21)-C(22)-C(14)	-2.9(5)
C(20)-C(21)-C(22)-C(14)	176.4(5)
C(16)-C(21)-C(22)-C(31)	111.6(5)
C(20)-C(21)-C(22)-C(31)	-69.1(7)
C(15)-C(14)-C(22)-C(23)	-52.7(6)
C(13)-C(14)-C(22)-C(23)	126.3(5)
C(15)-C(14)-C(22)-C(21)	-176.2(4)
C(13)-C(14)-C(22)-C(21)	2.8(5)
C(15)-C(14)-C(22)-C(31)	74.8(6)
C(13)-C(14)-C(22)-C(31)	-106.2(5)
C(21)-C(22)-C(23)-C(24)	58.9(6)
C(14)-C(22)-C(23)-C(24)	-57.7(6)
C(31)-C(22)-C(23)-C(24)	175.6(5)
C(22)-C(23)-C(24)-C(25)	-171.3(4)
C(23)-C(24)-C(25)-C(26)	-177.3(5)

C(24)-C(25)-C(26)-C(27)	-178.9(5)
C(25)-C(26)-C(27)-C(28)	-172.8(5)
C(26)-C(27)-C(28)-C(29)	179.0(5)
C(27)-C(28)-C(29)-C(30)	-176.7(5)
C(23)-C(22)-C(31)-C(32)	51.1(9)
C(21)-C(22)-C(31)-C(32)	174.3(7)
C(14)-C(22)-C(31)-C(32)	-77.6(8)
C(22)-C(31)-C(32)-C(33)	-173.7(6)
C(31)-C(32)-C(33)-C(34)	-70.8(9)
C(32)-C(33)-C(34)-C(35)	-168.7(6)
C(33)-C(34)-C(35)-C(36)	-179.3(5)
C(34)-C(35)-C(36)-C(37)	-178.7(6)
C(35)-C(36)-C(37)-C(38)	175.5(7)
C(45)-C(40)-C(41)-C(42)	0.2(9)
C(39)-C(40)-C(41)-C(42)	-179.8(5)
C(40)-C(41)-C(42)-C(43)	-0.7(9)
C(41)-C(42)-C(43)-C(44)	-0.1(9)
C(41)-C(42)-C(43)-C(46)	179.4(5)
C(42)-C(43)-C(44)-C(45)	1.5(8)
C(46)-C(43)-C(44)-C(45)	-178.0(5)
C(43)-C(44)-C(45)-C(40)	-2.1(9)
C(41)-C(40)-C(45)-C(44)	1.2(9)
C(39)-C(40)-C(45)-C(44)	-178.8(5)

Anisotropic displacement parameters ($Å^2 x\ 10^3$)for san590. The anisotropic displacement factor exponent takes the form: $-2p^2[\ h^2a^{*2}U^{11} + ... + 2\ h\ k\ a^*\ b^*\ U^{12}\ ]$

	U^{11}	U^{22}	U^{33}	U^{23}	U^{13}	U^{12}
C(1)	133(4)	117(4)	104(3)	-15(3)	7(3)	-63(4)
C(2)	92(3)	91(3)	91(3)	-2(2)	-8(2)	-43(3)
C(3)	103(3)	106(4)	127(4)	-5(3)	21(3)	-28(3)
C(4)	115(4)	79(3)	138(4)	-1(3)	16(3)	-21(3)
C(5)	96(2)	84(2)	112(2)	-2(1)	-11(2)	-36(1)
C(6)	96(2)	84(2)	112(2)	-2(1)	-11(2)	-36(1)
C(7)	125(4)	76(3)	165(5)	-23(3)	27(4)	-40(3)
C(8)	96(2)	84(2)	112(2)	-2(1)	-11(2)	-36(1)
C(9)	101(3)	80(3)	95(3)	5(2)	-23(2)	-34(2)
C(10)	92(3)	67(2)	94(3)	6(2)	-24(2)	-27(2)
C(11)	109(3)	64(2)	92(3)	-11(2)	-17(2)	-21(2)
C(12)	102(3)	72(2)	86(3)	-7(2)	-14(2)	-24(2)
C(13)	75(2)	67(2)	93(3)	-6(2)	-19(2)	-18(2)
C(14)	88(2)	64(2)	83(2)	-3(2)	-21(2)	-23(2)
C(15)	96(3)	65(2)	81(2)	0(2)	-19(2)	-16(2)
C(16)	80(3)	80(3)	115(3)	-2(2)	-21(2)	-30(2)
C(17)	105(3)	115(4)	130(4)	10(3)	-4(3)	-52(3)
C(18)	143(5)	152(6)	153(6)	1(5)	8(4)	-84(5)
C(19)	165(6)	148(6)	180(7)	10(5)	4(5)	-100(5)
C(20)	152(5)	99(4)	158(6)	-16(3)	-13(4)	-68(4)
C(21)	98(3)	86(3)	124(4)	-4(3)	-22(3)	-38(3)
C(22)	123(4)	70(2)	99(3)	-14(2)	-24(3)	-29(3)
C(23)	129(4)	73(3)	121(4)	-21(3)	-11(3)	-23(3)
C(24)	99(3)	83(3)	130(4)	-11(3)	0(3)	-15(3)
C(25)	111(4)	88(3)	131(4)	-2(3)	-10(3)	-20(3)
C(26)	110(4)	112(4)	113(4)	-2(3)	-17(3)	-25(3)
C(27)	103(4)	101(4)	141(5)	-1(3)	-8(3)	-18(3)
C(28)	106(3)	90(3)	117(4)	-5(3)	-13(3)	-19(3)
C(29)	106(4)	92(3)	118(4)	-7(3)	-13(3)	-20(3)

C(30)	133(5)	117(4)	138(5)	-11(4)	-33(4)	-30(4)
C(31)	174(6)	175(6)	112(4)	-50(4)	-9(4)	-77(6)
C(32)	183(7)	164(7)	191(8)	32(6)	-19(6)	-101(6)
C(33)	147(5)	147(5)	114(4)	4(4)	-37(4)	-67(5)
C(34)	153(5)	126(4)	107(4)	0(3)	-39(4)	-59(4)
C(35)	149(5)	145(5)	115(4)	10(4)	-32(4)	-81(5)
C(36)	189(7)	165(6)	98(4)	-4(4)	-23(4)	-97(6)
C(37)	210(9)	217(9)	120(5)	-1(5)	-38(5)	-124(8)
C(38)	176(7)	183(7)	150(6)	29(5)	-69(5)	-78(7)
N(1)	199(6)	129(4)	140(4)	-18(3)	32(4)	-101(4)
C(39)	122(4)	88(3)	155(5)	0(3)	-35(4)	-34(3)
C(40)	103(3)	69(3)	135(4)	8(3)	-20(3)	-33(3)
C(41)	122(4)	97(3)	125(4)	-13(3)	-25(3)	-19(3)
C(42)	115(4)	93(3)	125(4)	-18(3)	-10(3)	-4(3)
C(43)	85(3)	76(3)	115(4)	8(2)	1(2)	-29(2)
C(44)	107(4)	89(3)	134(4)	-6(3)	-31(3)	-28(3)
C(45)	113(4)	73(3)	141(4)	-17(3)	-27(3)	-17(3)
C(46)	89(3)	91(3)	112(4)	13(3)	6(3)	-27(3)
C(47)	90(3)	81(3)	111(3)	9(2)	-1(3)	-30(3)
C(48)	87(3)	77(3)	90(3)	7(2)	2(2)	-28(2)
C(49)	109(4)	87(3)	100(3)	-19(2)	13(3)	-35(3)
C(50)	114(4)	100(3)	87(3)	-16(2)	-6(3)	-45(3)
C(51)	90(3)	87(3)	70(2)	-5(2)	-4(2)	-44(2)
C(52)	83(2)	71(2)	69(2)	1(2)	-13(2)	-33(2)
C(53)	86(3)	82(3)	82(2)	1(2)	-6(2)	-33(2)
C(54)	88(3)	98(3)	74(2)	3(2)	-13(2)	-49(2)
C(55)	116(4)	149(5)	83(3)	1(3)	-23(3)	-72(4)
C(56)	93(3)	154(5)	101(4)	24(4)	-37(3)	-47(4)
C(57)	88(3)	123(4)	125(4)	36(4)	-31(3)	-39(3)
C(58)	93(3)	88(3)	96(3)	15(2)	-17(2)	-36(3)
C(59)	83(2)	85(3)	83(2)	12(2)	-16(2)	-43(2)
C(60)	85(2)	75(2)	80(2)	-3(2)	-11(2)	-35(2)
C(61)	96(3)	78(3)	105(3)	2(2)	-29(2)	-41(2)
C(62)	102(3)	104(3)	111(3)	5(3)	-12(3)	-57(3)
C(69)	95(3)	79(2)	81(3)	-8(2)	-12(2)	-30(2)
C(70)	120(3)	95(3)	77(3)	0(2)	-12(2)	-48(3)
C(71)	126(4)	117(4)	97(3)	1(3)	-2(3)	-54(3)
C(72)	155(5)	136(5)	115(4)	10(4)	-6(4)	-71(4)
N(2)	135(4)	108(4)	194(6)	4(4)	-73(4)	-15(3)
C(63)	193(4)	183(5)	160(3)	17(3)	-12(3)	-120(4)
C(64)	193(4)	183(5)	160(3)	17(3)	-12(3)	-120(4)
C(65)	193(4)	183(5)	160(3)	17(3)	-12(3)	-120(4)
C(66)	193(4)	183(5)	160(3)	17(3)	-12(3)	-120(4)
C(67)	193(4)	183(5)	160(3)	17(3)	-12(3)	-120(4)
C(68)	193(4)	183(5)	160(3)	17(3)	-12(3)	-120(4)
C(63A)	193(4)	183(5)	160(3)	17(3)	-12(3)	-120(4)
C(64A)	193(4)	183(5)	160(3)	17(3)	-12(3)	-120(4)
C(65A)	193(4)	183(5)	160(3)	17(3)	-12(3)	-120(4)
C(66A)	193(4)	183(5)	160(3)	17(3)	-12(3)	-120(4)
C(67A)	193(4)	183(5)	160(3)	17(3)	-12(3)	-120(4)
C(68A)	193(4)	183(5)	160(3)	17(3)	-12(3)	-120(4)
C(73)	218(7)	192(8)	161(5)	0(5)	31(5)	-124(7)
C(74)	218(7)	192(8)	161(5)	0(5)	31(5)	-124(7)
C(75)	218(7)	192(8)	161(5)	0(5)	31(5)	-124(7)
C(76)	218(7)	192(8)	161(5)	0(5)	31(5)	-124(7)
C(73A)	218(7)	192(8)	161(5)	0(5)	31(5)	-124(7)
C(74A)	218(7)	192(8)	161(5)	0(5)	31(5)	-124(7)
C(75A)	218(7)	192(8)	161(5)	0(5)	31(5)	-124(7)

C(76A)	218(7)	192(8)	161(5)	0(5)	31(5)	-124(7)

Figure S1. Crystal packing diagram of **DS** along the *c* axis.

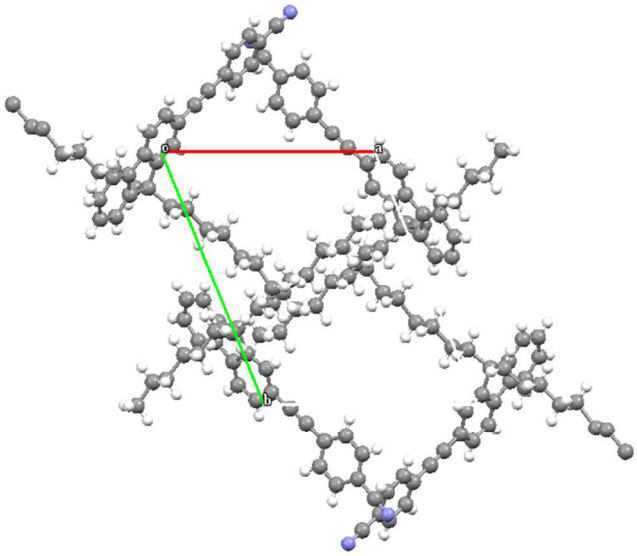

Computational details. Molecular geometry optimizations were obtained by Density Functional Theory (DFT) as performed in the Gaussian 09 code. For pK_a calculations zero point vibrational energies (ZPVE) were considered to account for thermal and entropic effects. The intramolecular charge transfer (ICT) properties of **DS**, **2DS** and **OS** were first analyzed by using TD-DFT with polarizable continuum model by using the integral equation formalism (for water). Hybrid functionals such as PBE0 have been found to be very accurate for CT parameters and excited states in charge transfer molecular systems. Then, we used the PBE0/6-31+G(d)/IEF-PCM [(a) Adamo, C.; Barone, V. Toward Reliable Density Functional Methods without Adjustable Parameters: The PBE0 Model. *J. Chem. Phys*. **1999**, *110*, 6158−6170. (b) Amovilli, C.; Barone, V.; Cammi, R.; Cancès, E.; Cossi, M.; Mennucci, B.; Pomelli, C. S.; Tomasi, J. Recent Advances in the Description of Solvent Effects with the Polarizable Continuum Model. *Adv. Quantum Chem*. **1998**, *32*, 227−261. (c) Tomasi, J.; Mennucci, B.; Cammi, R. Quantum Mechanical Continuum Solvation Models. *Chem. Rev*. **2005**, *105*, 2999−3094.] level of theory for the three

compounds and single electronic excitation by Natural Transition Orbital (NTO) analysis were carried out at the same level of theory.

Absorption	Hole	Electron
|1> ; 3.384 eV (366 nm); 84-85 ; w = 0.7 ; f = 1.403	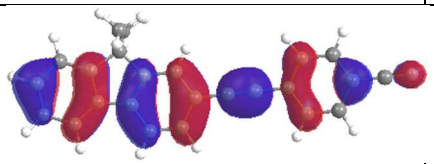	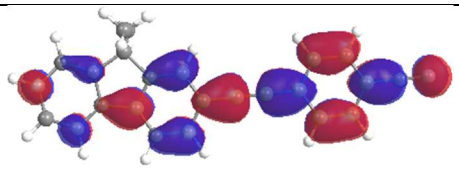
|1> ; 4.270 eV (290 nm) ; w = 0.48 ; f = 0.188	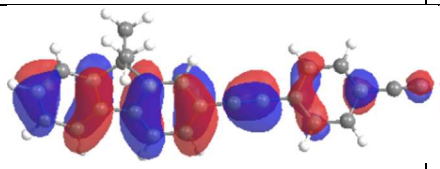	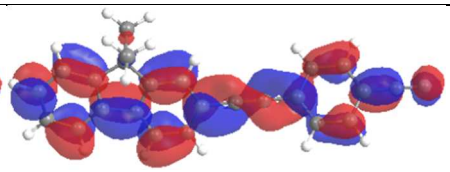
|1> ; 3.083 eV (402 nm); (252-253, *w* = 0.65 and 250-253, *w* = 0.43) f = 2.385	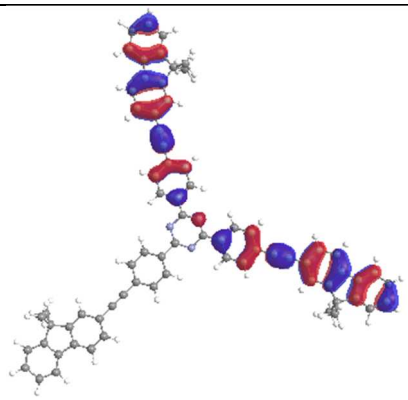	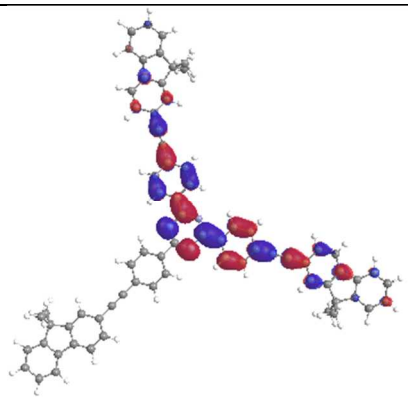
|1> ; 3.083 eV (402 nm); 252-254, *w* = 0.66 and 251-253, w = 0.43; f = 2.385	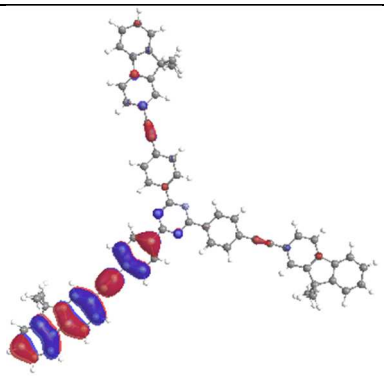	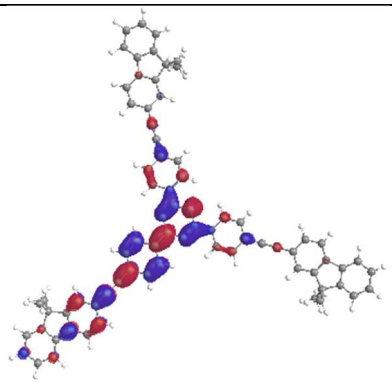

|1> ; **3.812 eV** (325 nm); **w = 0.95** ; **f = 0.592** **(251-255)**	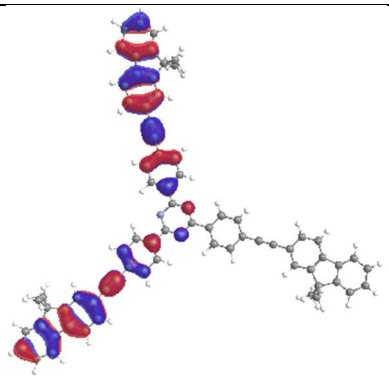	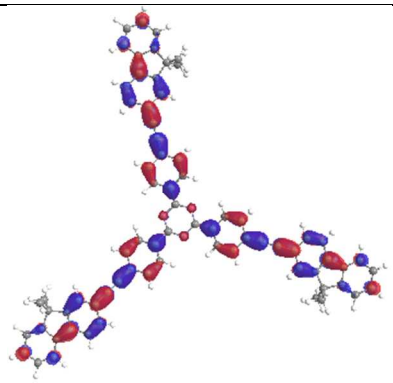

Figure S2. Natural transition orbitals and transition energy diagram for **DS** (left) and **OS** (right) illustrating the nature of the lowest-energy transition, computed at PBE0/6-31+G(d,p)/IEF-PCM-DMSO. The first column indicates the number of the excited state, its energy in eV and wavelength, the oscillator strength (f) and the NTO coefficient (*w*) representing the extent to which the electronic excitation can be written as a single excitation.

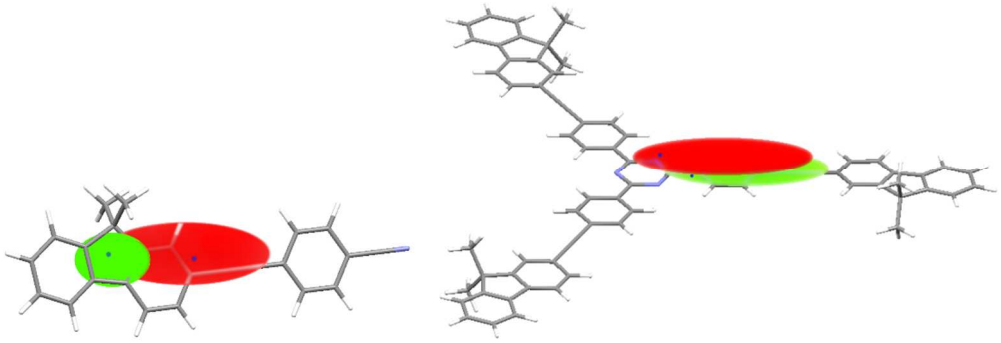

Figure S3. graphical representation of D_{CT}, and excess of electron density centroids (C_+ (r)/C_- (r) for **DS** (left) and **OS** (right).

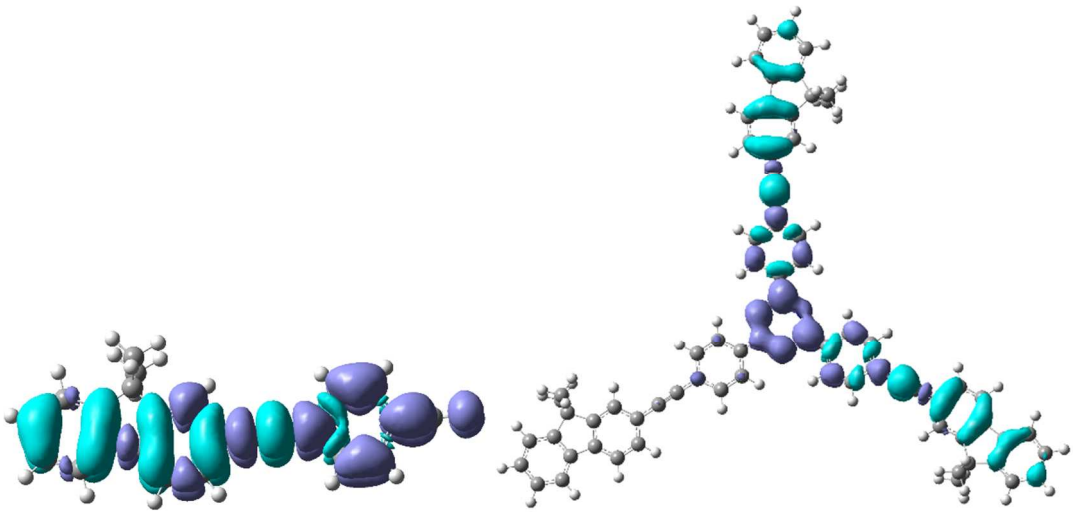

Figure S4. Electron density differences between electronic ground and first excited state for **DS** (left) and **OS** (right), computed at PBE0/6-31+G(d,p)/IEFPCM-DMSO, positive and negative variations of density are represented in purple and turquoise blue, respectively.

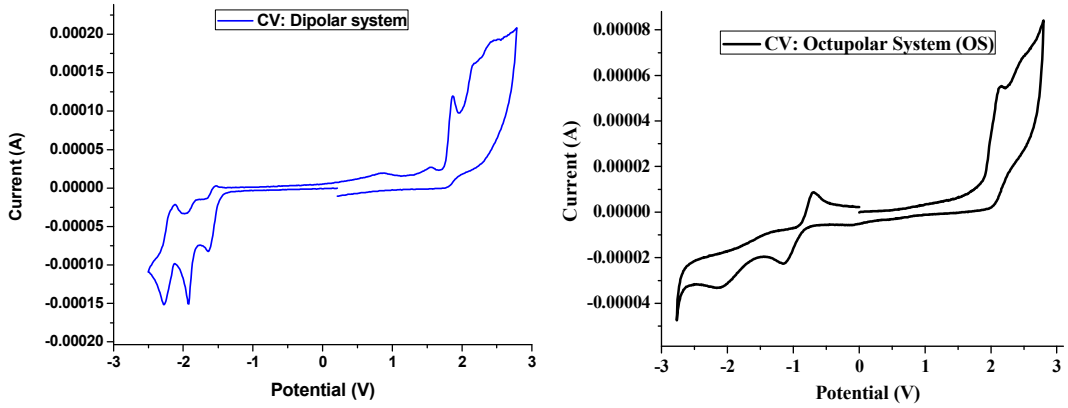

Figure S5. Cyclic voltammograms of 10 mM **DS** (left) and **OS** (right) in DMSO taken under N_2 atmosphere. Scan initiated at -3 V versus SCE in positive direction at 30 mV/s Platinum electrode area = 2.54 mm^2.

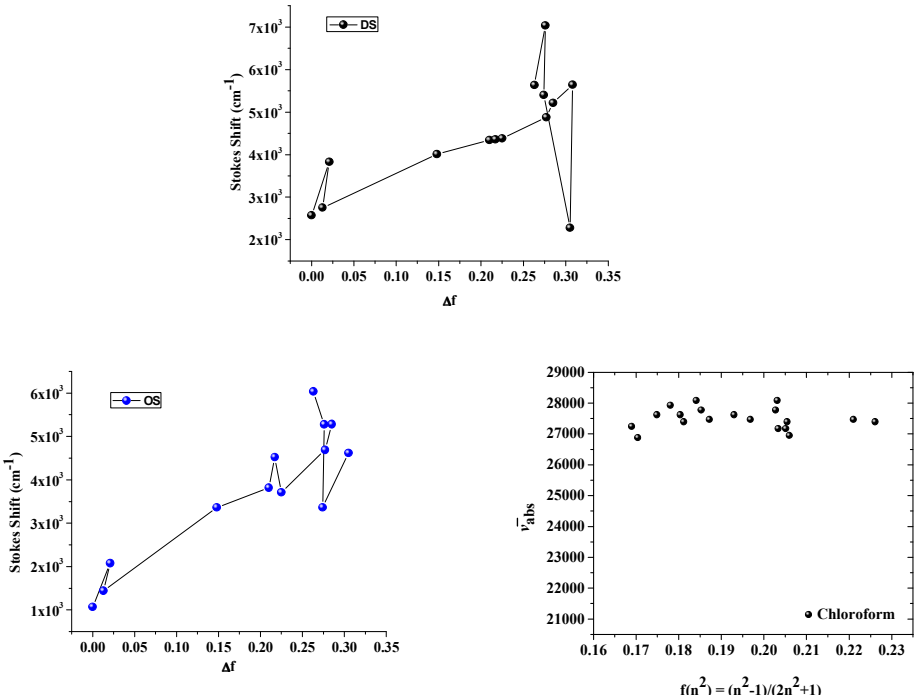

Figure S6. Lippert plots for compounds **DS** and **OS**.

Table S2. Catalán, Laurence and Kamlet-Taft solvent scales for compound **2DS**.

Catalán Solvent scale

	Observable	y_0 (cm^{-1})	a_{SA}	b_{SB}	c_{SP}	d_{SdP}	r
2DS	$\bar{\nu}_{abs}$	30014 ± 92	36 ± 58	-21 ± 35	-2177 ± 128	42 ± 28	0.98
	$\bar{\nu}_{cm}$	26140 ± 318	384 ±202	87 ± 120	-2106 ± 442	-174 ± 97	0.93
	$\Delta\bar{\nu}$	3874 ± 271	-348 ±172	-108 ± 102	-70 ± 377	216 ± 83	0.79

Laurence Solvent scale

	Observable	A0 (cm-1)	*a*	*b*	di	*e*	*r*
2DS	$\bar{\nu}_{abs}$	30419 ± 212	5 ± 47	82 ± 79	-2486 ± 269	-163 ± 78	0.96
	$\bar{\nu}_{em}$	29775 ± 2473	-1149 ± 553	870 ± 920	-6497 ± 3131	-839 ± 907	0.70
	$\Delta\bar{\nu}$	644 ± 2357	1154 ± 527	-788 ± 877	4010 ± 2984	676 ± 865	0.66

Kamlet-Taft solvent scale

	Observable	y_0 (cm^{-1})	*a*	*b*	*p*	*r*
2DS	$\bar{\nu}_{abs}$	28629 ± 108	125 ± 121	155 ± 151	-391 ± 165	0.65
	$\bar{\nu}_{em}$	25227 ± 554	-843 ± 662	635 ± 775	-1358 ± 845	0.58
	$\Delta\bar{\nu}$	3401 ± 506	969 ± 567	-479 ± 707	966 ± 770	0.58

Table S3. Photophysical properties of **2DS** in different solvents.[a]

				DS				
Solvent	***ε***	***n***	***Δf***	λ_a ***(nm)***	$\bar{\nu}_a$ ***(cm^{-1})***	λ_e ***(nm)***	$\bar{\nu}_e$ ***(cm^{-1})***	$\bar{\nu}_a - \bar{\nu}_e$ ***(cm^{-1})***
Hexane	2.02	1.4235	0	349	28653.295	403	24813.896	3839.40
Dioxane	2.22	1.4224	0.021	352	28409.09	406	24630.54	3778.55
Toluene	2.38	1.4961	0.013	353	28328.61	408	24509.80	3818.81
Chloroform	4.81	1.4459	0.148	353	28328.61	412	24271.84	4056.77
THF	7.52	1.4050	0.210	351	28490.028	406	24630.54	3859.49
DCM	8.93	1.4242	0.217	352	28409.09	408	24509.80	3899.29
Octanol	10.30	1.4295	0.225	351	28490.028	405	24691.358	3798.67
***i*-PrOH**	20.18	1.3776	0.277	349	28653.295	402	24875.62	3777.68
Acetone	21.01	1.3588	0.285	349	28653.295	406	24630.54	4022.76
MeOH	33.00	1.3288	0.308	348	28735.63	400	25000	3735.63
ACN	36.64	1.3442	0.305	349	28653.295	405	24691.358	3961.94
DMF	36.70	1.4305	0.274	353	28328.61	412	24271.84	4056.77

EG	41.40	1.4320	0.276	353	28328.61	458	21834.06	6494.55
DMSO	46.68	1.4793	0.263	354	28248.588	410	24390.24	3858.35

[a] Dielectric constant, (ε), refractive index, (n); Orientation polarizability, (Δf); absorption wavelength, (λ_a); absorption wavenumber, ($\bar{\nu}_a$); emission wavelength, (λ_e); emission wavenumber, ($\bar{\nu}_e$). Solvent notation: THF (tetrahydrofurane), DCM (dichloromethane), ACN (acetonitrile), DMF (dimethylformamide), DMSO (dimethyl sulfoxide).

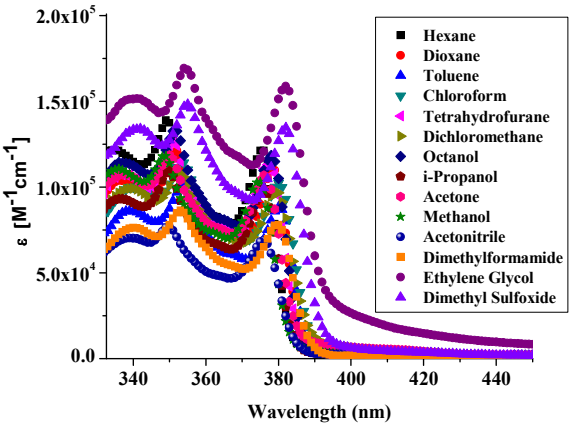

(A)

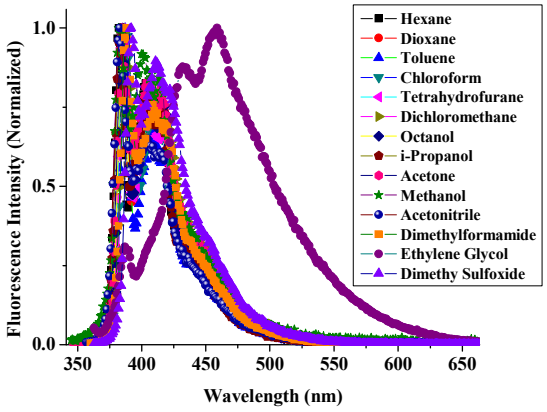

(B)

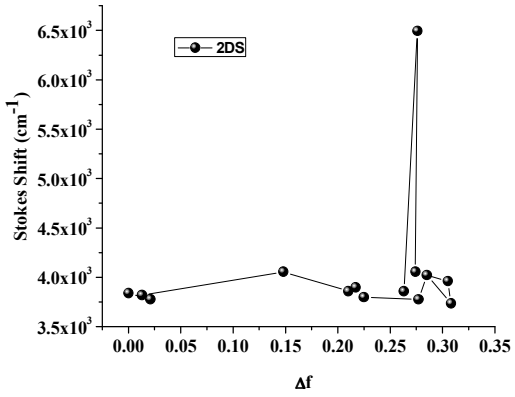

(C)

Figure S7. UV-Vis (A), Fluorescence (B) spectra and Lippert plot (C) for compound **2DS**.

Solvatochromic analysis for DS and OS.

More recently, an empirical methodology to explain experimental solvatochromic properties of chromophores from theoretical solvent characteristics was developed by Catalán.[1] It is well known that the relationship between solvent effects and spectral shifts can be denoted by a multilinear equation.[2] The mathematical treatment of solvent effects introduced by Catalán is based on four empirical and independent solvent scales.

$$y = y_0 + a_{SA}\,SA + b_{SB}\,SB + c_{SP}\,SP + d_{SdP}\,SdP \qquad (S1)$$

Here SA, SB, SP and SdP are the solvent acidity, basicity, polarizability and dipolarity properties, respectively, to the corresponding y observable. The coefficients a_{SA}, b_{SB}, c_{SP} and d_{SdP} represent the contribution of each type of interactions. Then, a Catalán solvent analysis was carried out in order to understand the solvent parameters that affect the photophysical properties ($\bar{\nu}_{abs}$, $\bar{\nu}_{em}$ and $\Delta\bar{\nu}$,) in **DS** and **OS**. The {SA, SB, SP, SdP} parameters for each solvent are taken from reference [1]. The regression coefficients y_o, a_{SA}, b_{SB}, c_{SP} and d_{SdP}, standard errors and the multilinear correlation coefficient, r, are presented in Table S4. In the case of $\bar{\nu}_{abs}$, good multilinear fit of 0.88 and 0.91 were

obtained for **DS** and **OS**, respectively. For **DS**, the analysis indicates that the major factors contributing to the solvatochromic changes in $\bar{\nu}_{abs}$ are mainly solvent polarizability, since the coefficient value c_{SP} is relatively large and has smaller standard error. However, the SdP parameter associated to dipolarity has some influence, because the multilinear regression without considering SdP gives a bit lower *r*-value according to Eq. 5, namely, 0.85 for {SA,SB,SP} variables, indicating that the solvent polarity factor cannot be neglected. In the case of **OS**, the analysis also indicates that the major factor contributing to the solvatochromic changes in $\bar{\nu}_{abs}$ is mainly the solvent polarizability. However, in this case, solvent acidity exerts an important influence too. The multilinear regression without considering SA gives significantly lower *r*-value according to Eq. S1, namely, 0.77 for {SB,SP,SdP} variables, indicating in this case that the solvent acidity parameter should not be neglected.

Table S4. Estimated coefficients y_0, a_{SA}, b_{SB}, c_{SP} and d_{SdP} for $\bar{\nu}_{abs}$, $\bar{\nu}_{em}$, and $\Delta\bar{\nu}$ (in cm^{-1}) and multiple correlation coefficient (*r*) for regression analysis of **DS** and **OS** according to the Catalán solvent parameters {SA, SB, SP, SdP}. Compound **2DS** is shown in Table S2, SI.

	Observable	y_0 (cm^{-1})	a_{SA}	b_{SB}	c_{SP}	d_{SdP}	*r*
DS	$\bar{\nu}_{abs}$	30197 ± 425	-637 ± 196	329 ± 174	**-2805 ± 586**	103 ± 148	0.88
	$\bar{\nu}_{em}$	31489 ± 1552	**-2524 ±716**	-799 ± 635	-5465 ± 2138	**-2157 ± 542**	0.94
	$\Delta\bar{\nu}$	-1291 ± 1651	1887 ±761	1129 ± 676	2659 ± 2273	**2260 ± 577**	0.92
OS	$\bar{\nu}_{abs}$	28942 ± 376	**-584 ± 184**	100 ± 142	**-1655 ± 521**	-266 ± 120	0.910
	$\bar{\nu}_{em}$	26153 ± 2385	-2220 ± 1172	-299 ± 904	-871 ± 3306	**-3730 ± 762**	0.921
	$\Delta\bar{\nu}$	2789 ± 2291	1636 ± 1125	399 ± 867	-784 ± 3175	**3464 ± 732**	0.910

In the case of $\bar{\nu}_{em}$ and $\Delta\bar{\nu}$ the largest values were also c_{SP} for **DS**, but d_{SdP} for **OS** gives the smallest standard error, indicating that the predominant factor influencing the solvatochromic changes in $\bar{\nu}_{em}$ and $\Delta\bar{\nu}$ are the solvent polarizability and polarity.

Similarly, we used the Kamlet-Taft empirical scale to verify the results obtained by Lippert-Mataga and Catalán analysis. Although Kamlet-Taft analysis describes the dipolarity/polarizability parameters in the same term, its reference point is cyclohexane, whereas Catalán analysis refers to the gas phase. Then we used Eq. S2:[2,3]

$$y = y_0 + a\,\alpha + b\,\beta + p\,\pi^* \qquad \text{(S2)}$$

where α, β and π^* are the acidity, basicity and polarity/polarizability solvent parameters, respectively. Table S5 shows the obtained multilinear regression coefficients and their standard errors.

Table S5. Estimated coefficients y_0, a, b and p for $\bar{\nu}_{abs}$, $\bar{\nu}_{em}$, and $\Delta\bar{\nu}$ (in cm^{-1}) and multiple correlation coefficient (r) for regression analysis of compounds **DS** and **OS** according to the Kamlet-Taft solvent parameters $\{\alpha, \beta$ and $\pi^*\}$.

	Observable	y_0 (cm^{-1})	*a*	*b*	*p*	*r*
DS	$\bar{\nu}_{abs}$	28498 ± 186	-183 ± 209	462 ± 261	**-510 ± 284**	0.60
	$\bar{\nu}_{em}$	27988 ± 528	-1514 ± 593	-1165 ± 739	**-2701 ± 806**	0.89
	$\Delta\bar{\nu}$	510 ± 508	1330 ± 570	1628 ± 711	**2191 ± 775**	0.89
OS	$\bar{\nu}_{abs}$	28017 ± 233	-365 ± 306	68 ± 328	**-572 ± 360**	0.62
	$\bar{\nu}_{em}$	25666 ± 714	-1673 ± 939	-1132 ± 1006	**-3430 ± 1104**	0.86
	$\Delta\bar{\nu}$	2351 ± 646	1307 ± 850	1200 ± 910	**2858 ± 999**	0.85

It can be noticed that Kamlet-Taft and Catalán analysis are in overall agreement, since solvent polarizability for absorbance and solvent polarity for emission and Stokes shift are the dominant parameters, here encompassed by π^*. However, Catalán analysis also

suggests that solvent acidity exerts an important influence and thus cannot be neglected. However, this result is not in full agreement with Kamlet-Taft regressions.

Then, we decide to incorporate a fourth solvatochromic analysis by using the new solvent scale proposed by Laurence, *et al.* [50, Main Text]. Due to the strong solvent effect observed for aprotic solvents, the interaction scheme should be better described with this solvent scale since acid and base parameters are not only a function of hydrogen bond interactions but Lewis acidity-basicity. Then we used Eq. S3:

$$A = A_0 + \text{di DI} + e\ \text{ES} + a\ \alpha_1 + b\ \beta_1 \qquad \text{(S3)}$$

where DI, ES, α_1 and β_1 are the dispersion-induction, electrostatic, Lewis acidity and hydrogen-bond basicity parameters, respectively; while di, *e*, *a* and *b* are the regression coefficients. Table S6 shows the obtained multilinear regression coefficients and their standard errors.

Table S6. Estimated coefficients A_0, di, *e*, *a* and *b* for $\bar{\nu}_{abs}$, $\bar{\nu}_{em}$, and $\Delta\bar{\nu}$ (in cm^{-1}) and multiple correlation coefficient (*r*) for regression analysis of compounds **DS** and **OS** according to the Laurence solvent parameters {α_1, β_1, DI and ES}.

	Observable	A_0 (cm^{-1})	*A*	*b*	di	*e*	*r*
DS	$\bar{\nu}_{abs}$	30805 ± 652	-348 ± 146	440 ± 242	**-3244 ± 825**	-218 ± 239	0.83
	$\bar{\nu}_{em}$	32142 ± 2688	-1304 ± 601	192 ± 1000	-5981 ± 3403	**-3241 ± 986**	0.88
	$\Delta\bar{\nu}$	-1337 ± 2668	955 ± 597	248 ± 992	2737 ± 3378	**3023 ± 979**	0.88
OS	$\bar{\nu}_{abs}$	29323 ± 613	-264 ± 140	219 ± 207	**-1963 ± 782**	**-524 ± 204**	0.84
	$\bar{\nu}_{em}$	26121 ± 3006	-964 ± 686	1304 ± 1019	-928 ± 3835	**-5176 ± 1004**	0.92
	$\Delta\bar{\nu}$	3201 ± 2830	699 ± 646	-1084 ± 959	-1035 ± 3611	**4652 ± 946**	0.91

A comparison of the three solvent scales reveals that correlation coefficients are better for Catalán scale which highlights the importance of solvent polarizability. Kamlet-Taft

analysis also reveals important charge transfer properties in both, **DS** and **OS** from the larger value of *p* ($\bar{\nu}_{em}$) compared to *p* ($\bar{\nu}_{abs}$), which is in agreement with Laurence scale due to the larger value of *e* ($\bar{\nu}_{em}$) compared to *e* ($\bar{\nu}_{abs}$). It is worth mentioning that in accordance to the four solvatochromic analyses, solvent polarizability and polarity are dominant, but this solvent dependence becomes more important in the excited state (parameters c_{SP}, d_{SdP}, *p*, di and *e* for $\bar{\nu}_{em}$). Interestingly, with the Laurence scale we realized that solvent acidity is not an influencing factor as it was suggested by Catalán scale. In fact, when we removed the amphiprotic solvents like alcohols, the $\bar{\nu}_{abs}$ and $\bar{\nu}_{em}$ Catalán correlations drastically improved to 0.97 and 0.95 for **DS** and, 0.92 and 0.93 for **OS**. Meanwhile, the $\bar{\nu}_{abs}$ and $\bar{\nu}_{em}$ Laurence correlations were improved to a lesser extent for **DS** and remains practically the same for **OS**. This highlights the similarity between α_1 and the Kamlet-Taft α parameter.[4] Moreover, although the excited state basicity for the nitrile and *s*-triazine groups of the respective **DS** and **OS** compounds must be stronger in the excited state (See density difference plots in Figure S4, above) due to the photoinduced ICT process, this effect is not clear since solvent acidity is not only an influencing factor for $\bar{\nu}_{em}$, but also for $\bar{\nu}_{abs}$.

From the above considerations we also realized that the relationship of $\bar{\nu}_{abs}$ *vs.* quadratic value of the high frequency polarizability function $f(n^2) = (n^2 - 1) / (2n^2 + 1)$, from the Lippert-Mataga relation, shows a linear trend ($r = 0.975$), which is in accordance with the empirical scales of Catalán, Kamlet-Taft and Laurence, indicating the existence of a relation between the absorption properties and the polarizability of the solvent. It is also to be noted that the obtained values of c_{SP} significantly differ (within experimental error) for absorption and emission, this is expected when no van der Waals type interactions with the solvent are taking place, suggesting that the electronic structure of the Franck-Condon and relaxed excited states is quite different. This observation is highly relevant since for a molecule with poor acid-base solvent interactions such as **DS** and **OS**, the Franck-Condon and relaxed excited states can only be different due to the strong rotational motion present in the phenylacetylene π-bridge.

References

(1) Catalán, J. Toward a Generalized Treatment of the Solvent Effect Based on Four Empirical Scales: Dipolarity (SdP, a New Scale), Polarizability (SP), Acidity (SA), and Basicity (SB) of the Medium. *J. Phys. Chem. B* **2009**, *113*, 5951–5960.

(2) Kamlet, M. J.; Abboud, J. L. M.; Abraham, M. H.; Taft, R. W. Linear Solvation Energy Relationships. 23. A Comprehensive Collection of the Solvatochromic Parameters, Pi*, .Alpha, and Beta, and Some Methods for Simplifying the Generalized Solvatochromic Equation. *J. Org. Chem.*, **1983**, *48*, 2877–2887.

(3) Taft, R. W.; Kamlet, M. J. The Solvatochromic Comparison Method. 2. The α-Scale of Solvent Hydrogen-Bond Donor (HBD) Acidities. *J. Am. Chem. Soc.* **1976**, *98*, 2886−2894.

(4) Cerón-Carrasco, J. P.; Jacquemin, D.; Laurence, C.; Planchat, A.; Reichardt, C.; Sraïdi, K. Determination of a Solvent Hydrogen-Bond Acidity Scale by Means of the Solvatochromism of Pyridinium-N Phenolate Betaine Dye 30 and PCM-TD-DFT Calculations. *J. Phys. Chem. B* **2014**, *118*, 4605−4614.